

## Bioactive Secolignans from *Peperomia dindygulensis*

Jian-lin Wu,<sup>†</sup> Na Li,<sup>\*,‡,§</sup> Toshiaki Hasegawa,<sup>†</sup> Jun-ichi Sakai,<sup>‡</sup> Tomokazu Mitsui,<sup>‡</sup> Hirotsugu Ogura,<sup>‡</sup> Takao Kataoka,<sup>‡</sup> Seiko Oka,<sup>||</sup> Miwa Kiuchi,<sup>||</sup> Akira Tomida,<sup>∇</sup> Takashi Turuo,<sup>#</sup> Minjie Li,<sup>†</sup> Wanxia Tang,<sup>†</sup> and Masayoshi Ando<sup>\*,‡</sup>

Graduate School of Science and Technology, Niigata University, 8050, 2-Nocho, Ikarashi, Niigata 950-2181, Japan, Department of Chemistry and Chemical Engineering, Niigata University, 8050, 2-Nocho, Ikarashi, Niigata 950-2181, Japan, The National Center for Drug Screening, Shanghai Institute of Materia Medica, Chinese Academy of Sciences, Guo Shou Jing Road 189, Zhanjiang High-Tech Park, Shanghai 201203, People's Republic of China, Center for Biological Resources and Informatics, Tokyo Institute of Technology, 4259 Nagatuta-cho, Midori-ku, Yokohama 226-8501, Japan, Center for Instrumental Analysis, Hokkaido University, Kita-12, Nishi-6, Sapporo 060-0812, Japan, Division of Genome Research, Cancer Chemotherapy Center, Japanese Foundation for Cancer Research 3-10-6, Ariake, Koto-ku, Tokyo 135-8550, Japan, and Institute of Molecular and Cellular Biosciences, University of Tokyo, Tokyo 113-0032, Japan

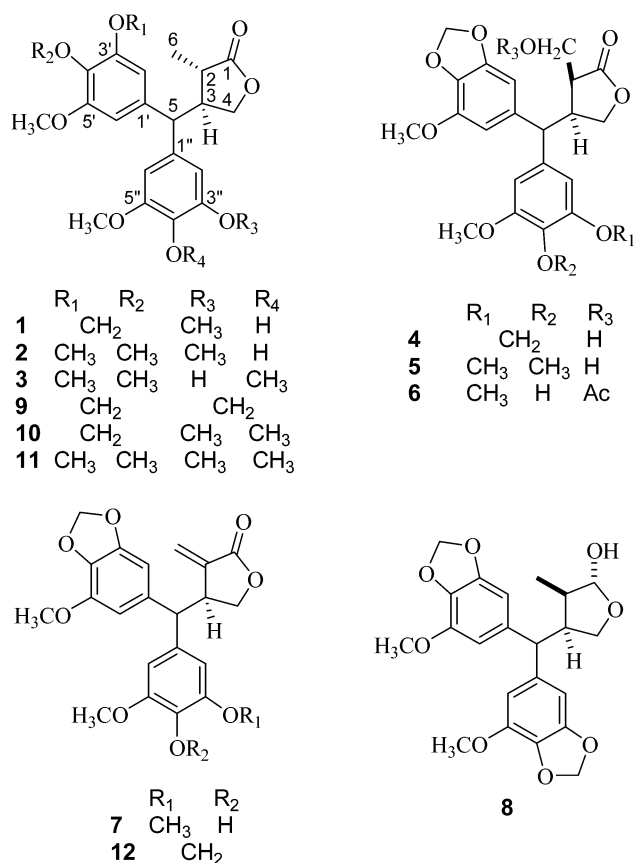
Received January 26, 2006

Thirteen secolignans, including eight new ones (**1–8**), were isolated from the EtOAc extract of *Peperomia dindygulensis*. The structures were mainly elucidated by 1D and 2D NMR and MS experiments, the relative configurations were determined by NOE correlations, and the absolute configurations were established by the optical rotations and CD spectra. Cytotoxicity and MDR (multidrug resistance) reversal activity of the isolated compounds were examined. Compounds **6** and **7**, peperomins B (**10**) and E (**12**), showed moderate to strong growth inhibitory activity against a malignant lung tumor cell (VA-13) with IC<sub>50</sub> values of 15.2, 13.5, 13.9, and 1.93 μM, respectively, and also inhibited the growth of a normal lung fibroblast cell (WI-38) at the same levels. Compound **7** and peperomin E (**12**) exhibited inhibitory activity against a liver tumor cell (HepG2) with IC<sub>50</sub> values of 22.3 and 12.1 μM. Compounds **5** and **7** and peperomins A, B, C, and E (**9–12**) enhanced calcein accumulation in MDR 2780 cells at 25 μg/mL. Compounds **2**, **3**, **7**, and peperomin E (**12**) showed inhibitory activity on induction of the intercellular adhesion molecule-1 (ICAM-1).

*Peperomia dindygulensis* C. DC. in Lecomte (Piperaceae) is used traditionally for the treatment of various types of cancer in the People's Republic of China.<sup>1</sup> Nine compounds were obtained from its EtOAc extract, including several compounds with cytotoxic activity, MDR (multidrug resistance) reversal activity, or anti-inflammatory activity in our previous investigation.<sup>2</sup> Thirteen secolignans, including eight new ones (**1–8**) and five known compounds, i.e., peperomins A, B, C,<sup>3</sup> E (**9–12**), and F,<sup>4</sup> were isolated in the further study of chemical constituents. The structures of the new compounds were established mainly by the analysis of NMR and mass spectra. Their relative configurations were determined by NOE correlations, and the absolute configurations by comparison of the optical rotations and CD spectra with those of known compounds. Cell growth inhibitory activity was evaluated on a normal lung fibroblast cell (WI-38), a malignant lung tumor cell (VA-13), and a liver tumor cell (HepG2). MDR reversal effects were screened by the accumulation of calcein in MDR 2780 cell lines. Anti-inflammatory activity was also measured by activity against induction of the intercellular adhesion molecule-1 (ICAM-1) induced by different signaling pathways mediated by TNF-α and IL-1α.

### Results and Discussion

Compound **1** had the molecular formula C<sub>22</sub>H<sub>24</sub>O<sub>8</sub> from the high-resolution EIMS. The IR spectrum showed absorption peaks of hydroxyl (3556 cm<sup>-1</sup>), γ-butyrolactone (1768 cm<sup>-1</sup>), and aromatic (1620 and 1456 cm<sup>-1</sup>) groups. The HMBC spectrum showed that four aromatic protons at δ 6.48 (1H, d, *J* = 1.5 Hz, H-2'), and



6.40 (1H, d, *J* = 1.5 Hz, H-6'), and 6.45 (2H, s, H-2'',6''), a methylenedioxy group attached to the aromatic ring at δ 5.94 (2H, s), three methoxy groups at δ 3.90 (3H, s) and 3.88 (6H, s), and one phenolic proton at δ 5.43 (1H, s) were attributed to a 5-methoxy-3,4-methylenedioxyphenyl and a 4-hydroxy-3,5-dimethoxyphenyl group. Three methine protons at δ 2.35 (1H, m, H-2), 2.88 (1H, m, H-3), and 3.60 (1H, d, *J* = 11.2 Hz, H-5), one oxymethylene at δ 4.31 (1H, dd, *J* = 7.6, 9.5 Hz, H-4a) and 3.83

\* To whom correspondence should be addressed. Tel: 86-21-50801313-138. Fax: 86-21-50800721. E-mail: nali9898@hotmail.com. Tel and Fax: +81-25-2627326. E-mail: mando@eng.niigata-u.ac.jp.

<sup>†</sup> Graduate School of Science and Technology, Niigata University.

<sup>‡</sup> Department of Chemistry and Chemical Engineering, Niigata University.

<sup>§</sup> The National Center for Drug Screening.

<sup>‡</sup> Tokyo Institute of Technology.

<sup>||</sup> Hokkaido University.

<sup>∇</sup> Japanese Foundation for Cancer Research.

<sup>#</sup> University of Tokyo.

**Table 1.**  $^1\text{H}$  NMR Data for Compounds **1–8** ( $\text{CDCl}_3$ , 500 MHz)<sup>a</sup>

proton	1	2	3	4	5	6	7	8
1								5.16 (1H, s)
2	2.35 (1H, m)	2.37 (1H, dq, 7.6, 7.3)	2.35 (1H, dq, 7.5, 7.3)	2.71 (1H, m)	2.71 (1H, m)	2.85 (1H, m)		2.22 (1H, dq, 6.4, 7.3)
3	2.88 (1H, m)	2.92 (1H, m)	2.91 (1H, m)	3.44 (1H, m)	3.49 (1H, m)	3.49 (1H, m)	3.78 (1H, m)	3.43 (1H, m)
4	4.31 (1H, dd, 7.6, 9.5)	4.29 (1H, dd, 7.8, 9.8)	4.32 (1H, dd, 7.6, 9.8)	4.07 (1H, dd, 8.8, 10.0)	4.11 (1H, dd, 8.8, 10.0)	4.08 (1H, dd, 8.1, 10.2)	4.33 (1H, dd, 7.8, 9.5)	3.85 (1H, m)
	3.83 (1H, dd, 7.6, 9.5)	3.86 (1H, m)	3.83 (1H, m)	4.04 (1H, dd, 8.5, 10.0)	4.04 (1H, dd, 8.5, 10.0)	4.00 (1H, dd, 9.0, 10.2)	4.01 (1H, dd, 4.6, 9.5)	3.59 (1H, dd, 5.9, 10.3)
5	3.60 (1H, d, 11.2)	3.63 (1H, d, 11.2)	3.60 (1H, d, 11.5)	4.04 (1H, d, 12.9)	4.08 (1H, d, 11.5)	3.72 (1H, d, 12.2)	3.68 (1H, d, 11.5)	3.58 (1H, m)
6	0.92 (3H, d, 7.3)	0.94 (3H, d, 7.3)	0.94 (3H, d, 7.3)	3.94 (1H, m)	3.93 (1H, dd, 3.2, 11.2)	4.29 (1H, dd, 3.7, 11.5)	6.13 (1H, d, 2.5)	0.86 (3H, d, 7.3)
				3.76 (1H, dd, 3.4, 11.0)	3.74 (1H, dd, 3.4, 11.2)	4.23 (1H, dd, 3.9, 11.5)	4.85 (1H, d, 2.5)	
2'	6.48 (1H, d, 1.5)	6.47 (1H, s)	6.47 (1H, s)	6.41 (1H, d, 1.7)	6.42 (1H, d, 1.5)	6.38 (1H, d, 1.5)	6.46 (1H, d, 1.5)	6.46 (1H, d, 1.5)
6'	6.40 (1H, d, 1.5)	6.47 (1H, s)	6.47 (1H, s)	6.39 (1H, d, 1.7)	6.41 (1H, d, 1.5)	6.33 (1H, d, 1.5)	6.40 (1H, d, 1.5)	6.40 (1H, d, 1.5)
2''	6.45 (1H, s)	6.49 (1H, s)	6.57 (1H, d, 2.0)	6.53 (1H, d, 1.6)	6.51 (1H, s)	6.49 (1H, s)	6.44 (1H, s)	6.59 (1H, d, 1.5)
6''	6.45 (1H, s)	6.49 (1H, s)	6.34 (1H, d, 2.0)	6.46 (1H, d, 1.6)	6.51 (1H, s)	6.49 (1H, s)	6.44 (1H, s)	6.48 (1H, d, 1.5)
OCH <sub>2</sub> O	5.94 (2H, s)			5.95 (1H, d, 1.5)	5.94 (1H, d, 1.5)	5.94 (1H, d, 1.5)	5.95 (2H, s)	5.92 (2H, s)
				5.94 (1H, d, 1.5)	5.92 (1H, d, 1.5)	5.92 (1H, d, 1.5)		5.91 (1H, d, 1.5)
				5.93 (1H, d, 1.5)				5.89 (1H, d, 1.5)
				5.91 (1H, d, 1.5)				
3'-OCH <sub>3</sub>		3.84 (3H, s)	3.85 (3H, s)					
4'-OCH <sub>3</sub>		3.81 (3H, s)	3.81 (3H, s)					
5'-OCH <sub>3</sub>	3.90 (3H, s)	3.84 (3H, s)	3.85 (3H, s)	3.90 (3H, s)	3.90 (3H, s)	3.90 (3H, s)	3.90 (3H, s)	3.89 (3H, s)
3''-OCH <sub>3</sub>	3.88 (3H, s)	3.89 (3H, s)			3.86 (3H, s)	3.89 (3H, s)	3.90 (3H, s)	
4''-OCH <sub>3</sub>			3.87 (3H, s)		3.82 (3H, s)			
5''-OCH <sub>3</sub>	3.88 (3H, s)	3.89 (3H, s)	3.85 (3H, s)	3.90 (3H, s)	3.86 (3H, s)	3.89 (3H, s)	3.90 (3H, s)	3.90 (3H, s)
3''-OH			5.80 (1H, br s)					
4''-OH	5.43 (1H, s)	5.43 (1H, br s)				5.45 (1H, s)	5.44 (1H, s)	
CH <sub>3</sub> CO						2.10 (3H, s)		

<sup>a</sup> Signals were assigned from the  $^1\text{H}$ - $^1\text{H}$  COSY, HMQC, and HMBC spectra.

(1H, dd,  $J = 7.6, 9.5$  Hz, H-4b), and one methyl at  $\delta$  0.92 (3H, d,  $J = 7.3$  Hz, H-6) remained in the  $^1\text{H}$  NMR spectrum.  $^1\text{H}$ - $^1\text{H}$  COSY correlations provided the linkages of C-6, C-2, C-3, C-4, and C-5. HMBC cross-peaks between the carbonyl carbon at  $\delta$  179.6 (C-1) and H-2, H-4a, and H-6 suggested the presence of a  $\gamma$ -butyrolactone group. The connections of the two phenyl groups with C-5 of the butyrolactone moiety were determined by the HMBC correlations of H-5 with C-1, C-2, and C-6 of the two phenyl groups and the EIMS base peak at  $m/z$  318. Thus, compound **1** is 2-methyl-3-[(5'-methoxy-3',4'-methylenedioxyphenyl)(4''-hydroxy-3'',5''-dimethoxyphenyl)methyl]butyrolactone. 2,3-*Trans* orientation was established from the NOE cross-peaks between H-2 and H-5, H-3 and H-6. The positive optical rotation, the positive Cotton effect at 278 nm, and the negative Cotton effect at 252 nm in the CD spectrum, similar to those of peperomin B, indicated the absolute configuration as 2*S*,3*S*.<sup>3</sup>

Compound **2** exhibited an ion peak at  $m/z$  432.1783 in the HREIMS, consistent with the molecular formula  $\text{C}_{23}\text{H}_{28}\text{O}_8$ . The IR spectrum indicated the presence of hydroxyl ( $3556\text{ cm}^{-1}$ ),  $\gamma$ -butyrolactone ( $1768\text{ cm}^{-1}$ ), and aromatic ( $1592$  and  $1454\text{ cm}^{-1}$ ) groups. It had proton and carbon signals similar to those of compound **1**, except for the 5-methoxy-3,4-methylenedioxyphenyl group (Tables 1 and 2). One methylenedioxy group disappearing and two additional methoxy groups appearing in **2** suggested that a 3,4,5-trimethoxyphenyl group existed. The EIMS base peak at  $m/z$  334 confirmed the existence of a (3,4,5-trimethoxyphenyl)(4-hydroxy-3,5-dimethoxyphenyl)methyl group. Optical rotation and CD spectrum similar to those of compound **1** established the

absolute configuration as 2*S*,3*S*. Thus, compound **2** is (2*S*,3*S*)-2-methyl-3-[(3',4',5'-trimethoxyphenyl)(4''-hydroxy-3'',5''-dimethoxyphenyl)methyl]butyrolactone.

Compound **3** had the same molecular formula as **2** ( $\text{C}_{23}\text{H}_{28}\text{O}_8$ ). The IR spectrum showed the hydroxyl,  $\gamma$ -butyrolactone, and aromatic groups. Its  $^1\text{H}$  and  $^{13}\text{C}$  NMR spectra were similar to those of compound **2**, except for the 4-hydroxy-3,5-dimethoxyphenyl group. Two nonequivalent aromatic protons [ $\delta$  6.57 (1H, d,  $J = 2.0$  Hz, H-2'') and 6.34 (1H, d,  $J = 2.0$  Hz, H-6'')] and two nonequivalent methoxy groups [ $\delta$  3.87 (3H, s) and 3.85 (3H, s)] were observed in the  $^1\text{H}$  NMR of **3**, instead of the signals of the symmetrical 4-hydroxy-3,5-dimethoxyphenyl group in **2**, so a 3-hydroxy-4,5-dimethoxyphenyl group existed in **3**. The 2*S*,3*S*-configuration was established from the optical rotation and CD spectrum.<sup>3</sup> Finally, compound **3** was established as (2*S*,3*S*)-2-methyl-3-[(3',4',5'-trimethoxyphenyl)(3''-hydroxy-4'',5''-dimethoxyphenyl)methyl]butyrolactone.

Compound **4** had the molecular formula  $\text{C}_{22}\text{H}_{22}\text{O}_9$  from HREIMS. The  $^1\text{H}$  NMR spectrum indicated the presence of two 5-methoxy-3,4-methylenedioxyphenyl groups. The remaining oxymethylene and three methines in the  $^1\text{H}$  NMR were ascribed to a  $\gamma$ -butyrolactone group from the  $^1\text{H}$ - $^1\text{H}$  COSY and HMBC spectra. In contrast to compounds **1–3**, the hydroxymethyl group, not the methyl group, was substituted at C-2 of compound **4**. The two 5-methoxy-3,4-methylenedioxyphenyl groups were connected at C-5 of the butyrolactone moiety as determined from the HMBC and the EIMS base peak at  $m/z$  315. Thus, the planar structure of compound **4** is 2-hydroxymethyl-3-[bis(5-methoxy-3,4-methylene-

**Table 2.**  $^{13}\text{C}$  NMR Data ( $\delta$ ) for Compounds **1–8** ( $\text{CDCl}_3$ , 125 MHz)<sup>a</sup>

carbon	1	2	3	4	5	6	7	8
1	179.6	179.6	179.7	178.9	179.0	176.7	170.8	105.0
2	40.3	40.2	40.2	44.9	45.1	42.1	135.9	41.5
3	47.3	47.4	47.2	41.8	41.8	41.9	42.6	43.1
4	70.4	70.4	70.4	72.5	72.5	72.0	69.7	71.2
5	56.2	56.4	56.5	49.9	50.1	50.2	55.4	50.6
6	15.9	15.8	15.9	60.6	60.6	61.3	124.9	11.2
1'	136.4	137.8	137.7	136.8	137.7	136.4	136.3	138.8
2'	101.1	104.8	104.8	100.9	101.0	100.9	101.1	101.4
3'	149.5	153.5	153.5	149.4	149.4	149.5	149.5	149.1
4'	134.3	137.3	137.5	134.2	134.2	134.4	134.3	133.8
5'	143.6	153.5	153.5	143.5	143.5	143.6	143.7	143.5
6'	107.9	104.8	104.8	107.3	107.5	107.5	108.1	107.4
1''	133.2	132.6	134.5	136.8	137.7	132.4	132.5	137.9
2''	104.4	104.4	106.5	100.9	104.1	103.8	104.9	101.1
3''	147.2	147.3	149.6	149.5	153.6	147.4	147.1	149.1
4''	134.0	134.1	134.5	134.2	136.7	134.1	133.9	133.8
5''	147.2	147.3	152.5	143.8	153.6	147.4	147.1	143.4
6''	104.4	104.4	104.0	107.2	104.1	103.8	104.9	106.9
OCH <sub>2</sub> O	101.5			101.5	101.5	101.5	101.5	101.3
3'-OCH <sub>3</sub>		56.2	56.3					
4'-OCH <sub>3</sub>		60.9	60.9					
5'-OCH <sub>3</sub>	57.0	56.2	56.3	56.9	56.9	57.1	57.0	56.9
3''-OCH <sub>3</sub>	56.4	56.5			56.3	56.5	56.0	
4''-OCH <sub>3</sub>			60.9		60.9			
5''-OCH <sub>3</sub>	56.4	56.5	56.0	56.9	56.3	56.5	56.0	56.8
COCH <sub>3</sub>						170.0		
CH <sub>3</sub> CO						21.0		

<sup>a</sup> Signals were assigned from the  $^1\text{H}$ - $^1\text{H}$  COSY, HMQC, and HMBC spectra.

dioxyphenyl)methyl]butyrolactone. The *cis*-configuration between H-2 and H-3 was established by their NOE cross-peak. It was levorotatory.

Compound **5** had the molecular formula  $\text{C}_{23}\text{H}_{26}\text{O}_9$  from HREIMS. The IR spectrum showed the presence of hydroxyl,  $\gamma$ -butyrolactone, and aromatic groups. The proton and carbon NMR resembled those of compound **4**. The significant difference was that one 5-methoxy-3,4-methylenedioxyphenyl was replaced by a 3,4,5-trimethoxyphenyl group. Thus, compound **5** is 2-hydroxy-methyl-3-[(5'-methoxy-3',4'-methylenedioxyphenyl)(3'',4'',5''-trimethoxyphenyl)methyl]butyrolactone. The NOE cross-peak between H-2 and H-3 indicated their *cis*-configuration. It was a levorotatory isomer. Chou et al.<sup>5</sup> synthesized a mixture of related diastereoisomers.

The molecular formula of compound **6** was determined as  $\text{C}_{24}\text{H}_{26}\text{O}_{10}$ . Compound **6** had NMR signals similar to those of compound **5**. The evident difference was the presence of acetyl signals, which correlated with H-6 in the HMBC. The hydroxyl group at C-6 was acetylated in compound **6**, which induced downfield shifts of H-2 and H-6 and an upfield shift of C-2. The 5-methoxy-3,4-methylenedioxyphenyl and 4-hydroxy-3,5-dimethoxyphenyl groups were evident from the HMBC and supported by the EIMS base peak at  $m/z$  317. Therefore, compound **6** is 2-acetoxymethyl-3-[(5'-methoxy-3',4'-methylenedioxyphenyl)(4''-hydroxy-3'',5''-dimethoxyphenyl)methyl]butyrolactone. The *cis*-configuration between H-2 and H-3 was determined by the NOESY spectrum. It was levorotatory.

The molecular formula of compound **7** was  $\text{C}_{22}\text{H}_{22}\text{O}_8$ . The presence of hydroxyl,  $\gamma$ -butyrolactone, and aromatic rings was supported by the bands at 3556, 1760, 1622, and 1456  $\text{cm}^{-1}$  in the IR spectrum. The (5-methoxy-3,4-methylenedioxyphenyl)(4-hydroxy-3,5-dimethoxyphenyl)methyl group was determined by comparison of  $^1\text{H}$  and  $^{13}\text{C}$  NMR with compound **1** and the EIMS base peak at  $m/z$  318. The methyl group at C-2 in **1** was substituted by a methylene in **7** by comparing their proton and carbon signals. Thus, compound **7** is a secolognan with a  $\alpha$ -methylene moiety. The absolute configuration was established as 3*S* on the basis of the Cotton effects in the CD spectrum, where a positive Cotton effect

**Table 3.** Cell Growth Inhibitory Effects of Compounds **1–12** against WI-38, VA-13, and HepG2 Cell Lines ( $\text{IC}_{50}$   $\mu\text{M}$ )<sup>a</sup>

compound	WI-38	VA-13	HepG2
<b>1</b>	174	112	159
<b>2</b>	184	151	163
<b>3</b>	>231	>231	>231
<b>4</b>	12.8	113	97.8
<b>5</b>	>224	>224	>224
<b>6</b>	14.8	15.2	75.9
<b>7</b>	20.9	13.5	22.3
<b>8</b>	142	138	140
<b>9</b>	>239	>239	>239
<b>10</b>	9.06	13.9	119
<b>11</b>	175	120	189
<b>12</b>	1.21	1.93	12.1
Taxol	0.0468	0.0059	9.49
ADM	1.21	0.699	2.21

<sup>a</sup> Cell growth inhibitory effects on three cells were determined, and  $\text{IC}_{50}$  was defined as the compound concentration causing 50% growth inhibition.

at 278 nm was followed by a negative Cotton effect at 250 nm, as in peperomin E.<sup>4</sup> Compound **7** is thus (3*S*)-2-methylene-3-[(5'-methoxy-3',4'-methylenedioxyphenyl)(4''-hydroxy-3'',5''-dimethoxyphenyl)methyl]butyrolactone.

Compound **8**,  $\text{C}_{22}\text{H}_{24}\text{O}_8$ , exhibited aromatic group absorptions in the IR spectrum. The bis(5-methoxy-3,4-methylenedioxyphenyl)-methyl group was determined by comparison of  $^1\text{H}$  and  $^{13}\text{C}$  NMR data with compound **4** and the EIMS base peak at  $m/z$  316. No carbonyl carbon was observed in the  $^{13}\text{C}$  NMR, and a proton [ $\delta$  5.16 (1H, s, H-1)] and carbon ( $\delta$  105.0, C-1) of the hemiacetal group appeared in the  $^1\text{H}$  and  $^{13}\text{C}$  NMR of **8**, respectively. Moreover, H-1 correlated with C-3, C-4, and C-6 in the HMBC spectrum, indicating that this compound was a tetrahydrofuran derivative. Thus, it is 2-methyl-3[bis(5-methoxy-3,4-methylenedioxyphenyl)methyl]tetrahydrofuran-1-ol. The NOE cross-peak between H-2 and H-3 indicated their *cis*-configuration. The singlet of H-1 suggested that the dihedral angle  $\text{H}_1-\text{C}_1-\text{C}_2-\text{H}_2$  was nearly  $90^\circ$ , which indicated a *trans*-orientation of H-1 and H-2.<sup>6</sup> It was a levorotatory isomer.

The cytotoxic activity of the isolated compounds except for peperomin F was examined on WI-38, VA-13, and HepG2 cell lines (Table 3). Among them, peperomin E (**12**) exhibited the strongest cell growth inhibitory activity against the malignant lung tumor cell (VA-13) with an  $\text{IC}_{50}$  value of 1.93  $\mu\text{M}$ , and compounds **6**, **7**, and peperomin B (**10**) showed inhibitory effects, with  $\text{IC}_{50}$  values of 15.2, 13.5, and 13.9  $\mu\text{M}$ , respectively. These compounds also inhibited the growth of normal lung fibroblast cells (WI-38) at the same levels. Compounds **7** and **12** showed inhibitory activity against the liver tumor cell (HepG2), and the  $\text{IC}_{50}$  values were 22.3 and 12.1  $\mu\text{M}$ , respectively.

One mechanism underlying MDR in mammalian tumor cells has been assigned to enhanced removal of drugs due to overexpression of efflux transporter proteins, such as P-glycoprotein (Pgp), the multidrug resistance proteins (MRP).<sup>7</sup> Thus, agents that inhibit these proteins could overcome the MDR effect. Calcein AM is used as an easily operated functional fluorescent probe for this drug efflux protein.<sup>8–10</sup> The MDR reversal effects of the isolated compounds except for peperomin F were examined on MDR 2780 cells using a known MDR reversal agent, verapamil, as a positive control (Table 4). Compounds **5**, **7**, and **9–12** enhanced calcein accumulation more than 120% compared to the control at 25  $\mu\text{g}/\text{mL}$ , although the effects were lower than that of verapamil.

Expression of excess amount of ICAM-1 on the surface of endothelial cells of a blood vessel plays an important role in the progress of inflammatory reaction.<sup>11–13</sup> The inhibitory effects on the induction of ICAM-1 of compounds **2–4**, **7**, and **9–12** were evaluated in the presence of IL-1 $\alpha$  using human A549 cells (lung carcinoma), and the cell viability was measured by an MTT assay

**Table 4.** Effects of Compounds **1–12** on the Accumulation of Calcein in MDR 2780 Cells<sup>a</sup>

compound	concentration, $\mu\text{g/mL}$	average of fluorescence/well <sup>b</sup>	% of control <sup>c</sup>	verapamil % <sup>d</sup>
control	0	3078		
verapamil	0.25	3273	106	100
	2.5	3574	116	100
	25	4632	150	100
<b>1</b>	0.25	3039	99	93
	2.5	3201	104	90
	25	3294	107	71
<b>2</b>	0.25	2947	96	90
	2.5	2936	95	82
	25	3165	103	68
<b>3</b>	0.25	3094	101	95
	2.5	3199	104	90
	25	3228	105	70
<b>4</b>	0.25	3007	98	92
	2.5	2929	95	82
	25	3223	105	70
<b>5</b>	0.25	3222	105	98
	2.5	3351	109	94
	25	3860	125	83
<b>6</b>	0.25	3310	108	101
	2.5	3192	104	89
	25	3195	104	69
<b>7</b>	0.25	3203	104	98
	2.5	3032	98	85
	25	3835	125	83
<b>8</b>	0.25	3039	99	93
	2.5	3201	104	90
	25	3294	107	71
<b>12</b>	0.25	3146	102	96
	2.5	3133	102	88
	25	4077	132	88
control	0	3888		
verapamil	0.25	3690	95	100
	2.5	4342	112	100
	25	5615	144	100
<b>9</b>	0.25	3312	85	90
	2.5	3554	91	82
	25	4658	120	83
control	0	2853		
verapamil	0.25	2396	84	100
	2.5	2778	97	100
	25	4280	150	100
<b>10</b>	0.25	3155	111	132
	2.5	2966	104	107
	25	3449	121	81
<b>11</b>	0.25	3104	109	130
	2.5	3286	115	118
	25	3950	138	92

<sup>a</sup> The amount of calcein accumulated in MDR human ovarian cancer 2780 cells was determined in the presence of 0.25, 2.5, and 25  $\mu\text{g/mL}$  of test compounds. <sup>b</sup> The values represent means of triplicate determination. <sup>c</sup> The values are the relative amount of calcein accumulated in the cell compared with the control experiment. <sup>d</sup> The values are expressed as the relative amount of calcein accumulated in the cell compared with that of verapamil.

(Table 5). Compounds **7** and **12** inhibited induction of ICAM-1 with  $\text{IC}_{50}$  values of 4.23 and 10.5  $\mu\text{M}$ , respectively. Although they showed cytotoxicity to A549 cells, the  $\text{IC}_{50}$  values (84.7 and 78.9  $\mu\text{M}$ ) were much higher than those of inhibition of ICAM-1. For compound **7**, the ratio was 20-fold. Compound **2** showed weaker inhibitory activity than compounds **7** and **12**, with an  $\text{IC}_{50}$  value of 44.3  $\mu\text{M}$ . In addition, the inhibitory effects of compounds **2**, **3**, **7**, and **11** on induction of ICAM-1 in the presence of TNF- $\alpha$  using A549 cells were also measured. Compound **7** showed evident inhibitory activity with an  $\text{IC}_{50}$  of 3.16  $\mu\text{M}$ , and compounds **2** and **3** showed weaker activity. Compounds **2** and **7** inhibited the induction of ICAM-1 induced by IL-1 $\alpha$  and TNF- $\alpha$  at the same level. The results suggest that these compounds block the common signaling pathway of NF- $\kappa\text{B}$  activation downstream of I $\kappa\text{B}$  kinase

activation, *de novo* RNA/protein synthesis of ICAM-1, or its intracellular transport to the plasma membrane.

## Experimental Section

**General Experimental Procedures.** Optical rotations were determined using a Horiba SEPA-200 polarimeter, and CD spectra were recorded on a JASCO J-720W spectrometer. IR and UV spectra were recorded on a Hitachi 270-30 spectrometer in  $\text{CHCl}_3$  and a JASCO V-550 UV/vis spectrophotometer in  $\text{CH}_3\text{OH}$ , respectively.  $^1\text{H}$  and  $^{13}\text{C}$  NMR spectra were run on a Varian UNITY-PS 500 spectrometer using  $\text{CDCl}_3$  as solvent. EIMS was recorded on a JEOL LMS-FABmate instrument, and HRESIMS on a Waters Q-ToF Micromass instrument. HPLC separation was performed on a Hitachi L-6200 HPLC instrument with an Inertsil Prep-sil GL 10  $\times$  250 mm column or an Inertsil Prep-ODS GL 10  $\times$  250 mm column, using Hitachi L-7400 UV and Shodex SE-61 RI detectors.

**Plant Material.** The whole plant of *P. dindygulensis* was collected from Yunnan Province, People's Republic of China, in February 2002. The plant was identified by Mr. Kaijiao Jiang, Kunming Institute of Botany. A voucher specimen (PDi-2002-2) has been deposited at the Faculty of Engineering, Niigata University, Japan.

**Extraction and Isolation.** The dried plant material (1.75 kg) was powdered and extracted three times (4 L/each) with MeOH at room temperature with the aid of a supersonic machine, and about 105 g of residue was obtained after evaporating the MeOH. The residue was suspended in  $\text{H}_2\text{O}$  and partitioned in sequence using hexane, EtOAc, and *n*-BuOH, respectively, to afford a hexane extract (40.7 g), an EtOAc extract (20.1 g), and an *n*-BuOH extract (15.6 g). The EtOAc extract was separated into 12 fractions ( $F_1$ – $F_{12}$ ) by column chromatography (CC) over silica gel.  $F_6$  (2.30 g) was subjected to silica gel CC, yielding seven subfractions ( $F_{6-1}$ – $F_{6-7}$ ), and peperomins E (**12**, 5.0 mg) and A (**9**, 895.0 mg) were purified from  $F_{6-4}$  and  $F_{6-5}$ , respectively, by normal-phase HPLC using hexane–EtOAc as solvent. Peperomin B (**10**, 79.7 mg) and compound **4** (5.8 mg) were obtained from  $F_7$  (3.52 g) using silica gel CC followed by normal-phase HPLC [hexane–EtOAc (55:45)].  $F_8$  (1.65 g) was divided into eight subfractions ( $F_{8-1}$ – $F_{8-8}$ ) by silica gel CC. Compounds **1** (2.3 mg), **7** (3.2 mg), and **8** (1.2 mg) were obtained from  $F_{8-4}$  using normal-phase HPLC [hexane–EtOAc (55:45)] and reversed-phase HPLC [MeOH– $\text{H}_2\text{O}$  (7:3 and 5:5)]. Peperomin C (**11**, 38.7 mg) and compound **3** (5.5 mg) were isolated from  $F_{8-5}$  with normal-phase HPLC [hexane–EtOAc (55:45)]. Peperomin F (24.9 mg) was obtained from  $F_{8-6}$  using HPLC [hexane–EtOAc (55:45)].  $F_{8-7}$  yielded compounds **6** (2.9 mg) and **5** (33.8 mg) with HPLC [hexane–EtOAc (55:45)] and repeated reversed-phase HPLC [MeOH– $\text{H}_2\text{O}$  (7:3)].  $F_{8-8}$  afforded compound **2** (8.8 mg) using normal-phase [hexane–EtOAc (55:45)] and reversed-phase HPLC [MeOH– $\text{H}_2\text{O}$  (7:3)].

**(2S,3S)-2-Methyl-3-[(5'-methoxy-3',4'-methylenedioxyphenyl)(4'-hydroxy-3'',5''-dimethoxyphenyl)methyl]butyrolactone (1):** pale yellow gum;  $[\alpha]_{\text{D}}^{20} +62.0$  (*c* 0.130,  $\text{CHCl}_3$ ); UV (MeOH)  $\lambda_{\text{max}}$  212, 245, 283 nm; CD (*c* 1 mM, MeOH)  $[\theta]_{278} +8061$ ,  $[\theta]_{252} -2064$ ; IR ( $\text{CHCl}_3$ )  $\nu_{\text{max}}$  3556, 2944, 1768, 1620, 1456, 1324, 1226, 1216, 1116  $\text{cm}^{-1}$ ;  $^1\text{H}$  NMR ( $\text{CDCl}_3$ , 500 MHz) and  $^{13}\text{C}$  NMR ( $\text{CDCl}_3$ , 125 MHz) data, see Tables 1 and 2; EIMS  $m/z$  417  $[\text{M} + \text{H}]^+$  (15), 416  $[\text{M}]^+$  (66), 318 (100), 287 (17); HREIMS  $m/z$  416.1476 (calcd for  $\text{C}_{22}\text{H}_{24}\text{O}_8$ , 416.1471).

**(2S,3S)-2-Methyl-3-[(3',4',5'-trimethoxyphenyl)(4'-hydroxy-3'',5''-dimethoxyphenyl)methyl]butyrolactone (2):** pale yellow gum;  $[\alpha]_{\text{D}}^{20} +41.5$  (*c* 0.440,  $\text{CHCl}_3$ ); UV (MeOH)  $\lambda_{\text{max}}$  212, 245, 274 nm; CD (*c* 1 mM, MeOH)  $[\theta]_{282} +8764$ ,  $[\theta]_{250} -6795$ ; IR ( $\text{CHCl}_3$ )  $\nu_{\text{max}}$  3556, 3032, 2944, 1768, 1592, 1454, 1420, 1328, 1238, 1214, 1118, 1018  $\text{cm}^{-1}$ ;  $^1\text{H}$  NMR ( $\text{CDCl}_3$ , 500 MHz) and  $^{13}\text{C}$  NMR ( $\text{CDCl}_3$ , 125 MHz) data, see Tables 1 and 2; EIMS  $m/z$  433  $[\text{M} + \text{H}]^+$  (15), 432  $[\text{M}]^+$  (56), 334 (100), 333 (58); HREIMS  $m/z$  432.1783 (calcd for  $\text{C}_{23}\text{H}_{28}\text{O}_8$ , 432.1784).

**(2S,3S)-2-Methyl-3-[(3',4',5'-trimethoxyphenyl)(3''-hydroxy-4''5''-dimethoxyphenyl)methyl]butyrolactone (3):** pale yellow gum;  $[\alpha]_{\text{D}}^{20} +14.5$  (*c* 0.275,  $\text{CHCl}_3$ ); UV (MeOH)  $\lambda_{\text{max}}$  212, 246, 279 nm; CD (*c* 1 mM, MeOH)  $[\theta]_{278} +4868$ ,  $[\theta]_{249} -814$ ; IR ( $\text{CHCl}_3$ )  $\nu_{\text{max}}$  3540, 3028, 1766, 1592, 1460, 1330, 1240, 1126, 1000  $\text{cm}^{-1}$ ;  $^1\text{H}$  NMR ( $\text{CDCl}_3$ , 500 MHz) and  $^{13}\text{C}$  NMR ( $\text{CDCl}_3$ , 125 MHz) data, see Tables 1 and 2; EIMS  $m/z$  433  $[\text{M} + \text{H}]^+$  (9), 432  $[\text{M}]^+$  (38), 334 (55), 333 (100); HREIMS  $m/z$  432.1786 (calcd for  $\text{C}_{23}\text{H}_{28}\text{O}_8$ , 432.1784).

**(-)-2,3-cis-2-Hydroxymethyl-3-[bis(5-methoxy-3,4-methylenedioxyphenyl)methyl]butyrolactone (4):** pale yellow gum;  $[\alpha]_{\text{D}}^{20} -42.2$

**Table 5.** Inhibitory Effect of Compounds on Induction of ICAM-1 and Cell Viability<sup>a</sup>

		2	3	4	7	9	10	11	12
ICAM-1 IC <sub>50</sub> (μM) <sup>b</sup>	IL-1α	44.3	119	>316	4.23	>316	>316	246	10.5
	TNF-α	29.0	59.9		3.16			125	
MTT IC <sub>50</sub> (μM) <sup>c</sup>		>316	>316	>316	84.7	>316	>316	>316	78.9

<sup>a</sup> A549 cells were pretreated with various concentrations of compounds for 1 h and then incubated in the presence of IL-1α or TNF-α for 6 h.

<sup>b</sup> Expression of ICAM-1 (% of control) was calculated by using the formula in the Experimental Section and used for determination of IC<sub>50</sub>. <sup>c</sup> A549 cells were incubated with serial dilutions of the compounds for 24 h. Cell viability (%) was measured by MTT assay and used for determination of IC<sub>50</sub>.

(*c* 1.120, CHCl<sub>3</sub>); UV (MeOH) λ<sub>max</sub> 212, 250, 283 nm; CD (*c* 1 mM, MeOH) [θ]<sub>284</sub> -5505, [θ]<sub>254</sub> +9350; IR (CHCl<sub>3</sub>) ν<sub>max</sub> 3028, 1766, 1318, 1232, 1218, 1096 cm<sup>-1</sup>; <sup>1</sup>H NMR (CDCl<sub>3</sub>, 500 MHz) and <sup>13</sup>C NMR (CDCl<sub>3</sub>, 125 MHz) data, see Tables 1 and 2; EIMS *m/z* 430 [M]<sup>+</sup> (38), 412 (14), 315 (100); HREIMS *m/z* 430.1269 (calcd for C<sub>22</sub>H<sub>22</sub>O<sub>9</sub>, 430.1264).

(-)-**2,3-cis-2-Hydroxymethyl-3-[(5'-methoxy-3',4'-methylenedioxyphenyl)(3'',4'',5''-trimethoxyphenyl)methyl]butyrolactone (5)**: pale yellow gum; [α]<sub>D</sub><sup>20</sup> -75.4 (*c* 0.180, CHCl<sub>3</sub>); UV (MeOH) λ<sub>max</sub> 212, 249, 281 nm; CD (*c* 1 mM, MeOH) [θ]<sub>280</sub> -6848, [θ]<sub>251</sub> +15286; IR (CHCl<sub>3</sub>) ν<sub>max</sub> 3268, 2944, 1762, 1592, 1456, 1328, 1224, 1126, 1010 cm<sup>-1</sup>; <sup>1</sup>H NMR (CDCl<sub>3</sub>, 500 MHz) and <sup>13</sup>C NMR (CDCl<sub>3</sub>, 125 MHz) data, see Tables 1 and 2; EIMS *m/z* 446 [M]<sup>+</sup> (13), 428 (29), 332 (82), 331 (100); HREIMS *m/z* 446.1573 (calcd for C<sub>23</sub>H<sub>26</sub>O<sub>9</sub>, 446.1576).

(-)-**2,3-cis-2-Acetoxyethyl-3-[(5'-methoxy-3',4'-methylenedioxyphenyl)(4''-hydroxy-3'',5''-dimethoxyphenyl)methyl]butyrolactone (6)**: pale yellow gum; [α]<sub>D</sub><sup>20</sup> -44.0 (*c* 0.145, CHCl<sub>3</sub>); UV (MeOH) λ<sub>max</sub> 214, 250, 280 nm; CD (*c* 1 mM, MeOH) [θ]<sub>282</sub> -11090, [θ]<sub>253</sub> +20240; IR (CHCl<sub>3</sub>) ν<sub>max</sub> 3556, 2948, 1774, 1618, 1456 1232, 1218, 1106 cm<sup>-1</sup>; <sup>1</sup>H NMR (CDCl<sub>3</sub>, 500 MHz) and <sup>13</sup>C NMR (CDCl<sub>3</sub>, 125 MHz) data, see Tables 1 and 2; EIMS *m/z* 415 [M - CH<sub>3</sub>COO]<sup>+</sup> (4), 414 [M - CH<sub>3</sub>COOH]<sup>+</sup> (15), 317 (100); HRESIMS *m/z* 497.1425 (calcd for [C<sub>24</sub>H<sub>26</sub>O<sub>10</sub>+Na]<sup>+</sup>, 497.1424).

(**3S**)-**2-Methylene-3-[(5'-methoxy-3',4'-methylenedioxyphenyl)(4''-hydroxy-3'',5''-dimethoxyphenyl)methyl]butyrolactone (7)**: pale yellow gum; [α]<sub>D</sub><sup>20</sup> +20.8 (*c* 0.170, CHCl<sub>3</sub>); UV (MeOH) λ<sub>max</sub> 213, 250, 280 nm; CD (*c* 1 mM, MeOH) [θ]<sub>278</sub> +10969, [θ]<sub>250</sub> -4349; IR (CHCl<sub>3</sub>) ν<sub>max</sub> 3556, 3036, 2948, 1760, 1622, 1456, 1324, 1230, 1210, 1116 cm<sup>-1</sup>; <sup>1</sup>H NMR (CDCl<sub>3</sub>, 500 MHz) and <sup>13</sup>C NMR (CDCl<sub>3</sub>, 125 MHz) data, see Tables 1 and 2; EIMS *m/z* 415 [M + H]<sup>+</sup> (13), 414 [M]<sup>+</sup> (52), 318 (100), 317 (32); HREIMS *m/z* 414.1313 (calcd for C<sub>22</sub>H<sub>22</sub>O<sub>8</sub>, 414.1314).

(-)-**1,2-trans-2,3-cis-2-Methyl-3[bis(5-methoxy-3,4-methylenedioxyphenyl)methyl]tetrahydrofuran-1-ol (8)**: pale yellow gum; [α]<sub>D</sub><sup>20</sup> -110.7 (*c* 0.030, CHCl<sub>3</sub>); UV (MeOH) λ<sub>max</sub> 216, 249, 280 nm; CD (*c* 1 mM, MeOH) [θ]<sub>280</sub> -9111, [θ]<sub>252</sub> +14041; IR (CHCl<sub>3</sub>) ν<sub>max</sub> 2948, 1634, 1494, 1454, 1432, 1216, 1212, 1132, 1092, 1046 cm<sup>-1</sup>; <sup>1</sup>H NMR (CDCl<sub>3</sub>, 500 MHz) and <sup>13</sup>C NMR (CDCl<sub>3</sub>, 125 MHz) data, see Tables 1 and 2; EIMS *m/z* 417 [M + H]<sup>+</sup> (8), 416 [M]<sup>+</sup> (30), 398 (43), 316 (100); HREIMS *m/z* 416.1476 (calcd for C<sub>22</sub>H<sub>24</sub>O<sub>8</sub>, 416.1471).

**Growth Inhibitory Activity to WI-38, VA-13, and HepG2 Cells in Vitro.** The cell lines were available from the Institute of Physical and Chemical Research (RIKEN), Tsukuba, Ibaraki, Japan. WI-38 and VA-13 cells were maintained in Eagle's MEM medium (Nissui Pharmaceutical Co., Tokyo, Japan) and RITC 80-7 medium (Asahi Technoglass Co., Chiba, Japan), respectively, both supplemented with 10% (v/v) fetal bovine serum (FBS) (Filtron PTY Ltd., Australia) with 80 μg/mL of kanamycin. HepG2 cells were maintained in D-MEM medium (Invitrogen, Carlsbad, CA) supplemented with 10% (v/v) FBS (Filtron PTY Ltd., Australia) with 80 μg/mL of kanamycin. The activity was measured as previously described.<sup>2</sup>

**Cellular Accumulation of Calcein.** MDR ovarian cancer A2780 cells (AD10) were maintained in PRMI-1640 medium (Invitrogen, Carlsbad, CA) supplemented with 10% (v/v) FBS (Filtron PTY Ltd., Australia) with 80 μg/mL of kanamycin. The activity was measured as previously described.<sup>14</sup>

**Inhibitory Activity on Induction of ICAM-1.** A549 cells were maintained in RPMI 1640 medium (Invitrogen, Carlsbad, CA) supplemented with 10% (v/v) FBS (JRH Bioscience, Lenexa, KS), and a penicillin-streptomycin antibiotic mixture (Invitrogen). Mouse anti-human ICAM-1 antibody C167 was purchased from Leinco Technologies, Inc. (Ballwin, MO), and peroxidase-conjugated goat anti-mouse IgG antibody was obtained from Jackson Immuno Research Laboratories, Inc. (West Grove, PA). Recombinant IL-1α and TNF-α were provided by Dainippon Pharmaceutical Co. Ltd. (Osaka Japan).

Cell surface expression of ICAM-1 and cell viability on the basis of MTT assay were measured as previously described.<sup>2</sup> Expression of ICAM-1 (% of control) was calculated as [(absorbance with sample and IL-1α/TNF-α treatment - absorbance without IL-1α/TNF-α treatment)/(absorbance with IL-1α/TNF-α treatment - absorbance without IL-1α/TNF-α treatment)] × 100. Cell viability (%) was calculated as [(experimental absorbance - background absorbance)/(control absorbance - background absorbance)] × 100.

**Acknowledgment.** This research was supported by the Japanese Society for the Promotion of Science (No. 13001288).

## References and Notes

- Jiangsu New Medical College. *Dictionary of Chinese Herbal Drugs*; Shanghai Science and Technology Press: Shanghai, 1978; p 622.
- Wu, J. L.; Li, N.; Hasegawa, T.; Sakai, J.; Kakuta, S.; Tang, W. X.; Oka, S.; Kiuchi, M.; Ogura, H.; Kataoka, T.; Tomida, A.; Tsuruo, T.; Ando, M. *J. Nat. Prod.* **2005**, *68*, 1656-1660.
- Chen, C. M.; Jan, F. Y.; Chen, M. T.; Lee, T. J. *Heterocycles* **1989**, *29*, 411-414.
- Govindachari, T. R.; Kumari, G. N. K.; Partho, P. D. *Phytochemistry* **1998**, *49*, 2129-2131.
- Chou, S. Y.; Wang, S. S.; Tsai, H. J.; Chen, S. F.; Ku, H. U.S. Patent 5,981,577, 1999.
- Rehberg, N.; Magnusson, G. *J. Org. Chem.* **1990**, *55*, 4340-4349.
- Wortelboer, H. M.; Usta, M.; van Zanden, J. J.; van Bladeren, P. J.; Rietjens, I. M. C. M.; Cnubben, N. H. P. *Biochem. Pharmacol.* **2005**, *69*, 1879-1890.
- Eneroth, A.; Åström, E.; Hoogstraate, J.; Schrenk, D.; Conrad, S.; Kauffmann, H. M.; Gjellan, K. *Eur. J. Pharm. Sci.* **2001**, *12*, 205-214.
- Tsuruo, T.; Iida-Saito, H.; Kawabata, H.; Oh-hara, T.; Hamada, H.; Utakoji, T. *Jpn. J. Cancer Res. (Gann)* **1986**, *77*, 682-692.
- Jonsson, B. Liminga, G.; Csoka, K.; Fridborg, H.; Dhar, S.; Nygren, P.; Larsson, R. *Eur. J. Cancer* **1996**, *32A* (5), 883-887.
- Kawai, S.; Kataoka, T.; Sugimoto, H.; Nakamura, A.; Kobayashi, T.; Arao, K.; Higuchi, Y.; Ando, M.; Nagai, K. *Immunopharmacology* **2000**, *48*, 129-135.
- Yuuya, S.; Hagiwara, H.; Suzuki, T.; Ando, M.; Yamada, A.; Suda, K.; Kataoka, T.; Nagai, K. *J. Nat. Prod.* **1999**, *62*, 22-30.
- Higuchi, Y.; Shimoma, F.; Koyanagi, R.; Suda, K.; Mitui, T.; Kataoka, T.; Nagai, K.; Ando, M. *J. Nat. Prod.* **2003**, *66*, 588-594.
- Li, N.; Wu, J.; Hasegawa, T.; Sakai, J.; Wang, L.; Kakuta, S.; Furuya, Y.; Tomida, A.; Tsuruo, T.; Ando, M. *J. Nat. Prod.* **2006**, *69*, 234-239.

NP0600447